

Non-proportional Loading Behavior of Elastoplastic Solids

S. Tsutsumi¹, K. Hashiguchi², M. Toyosada¹, K. Gotoh¹

Summary

In order to clarify the indispensable factors in elastoplastic constitutive equations for the description of general non-proportional loading behavior of soils, the mechanical responses to the stress probe test and the principal stress axes rotation are examined by numerical experiments and comparisons with test data. The necessity of the incorporation of both the vertex effect or the tangent effect, i.e. the inelastic stretching due to the stress rate tangential to the yield surface and the anisotropy in yield condition, both of which lead to the non-coaxiality, are revealed for the description of general loading behavior of soils.

Introduction

The traditional plastic constitutive equation having neither the vertex (tangent) effect nor the anisotropy in yield condition is capable of describing the deformation behavior for the stress path near the proportional loading. However, the stress path often deviates severely from the proportional loading in many real situations, e.g. the tidal waves, earthquakes, wheel rotation, footing penetration and the plastic instability phenomena inducing a shear band and/or a diffuse mode. It has been found experimentally for the non-proportional loading behavior of soils that not only the magnitude but also the direction of inelastic stretching is dependent on the direction of stress rate as was revealed in the stress probe test [1]. Further, inelastic deformation is induced by the principal stress axes rotation, even if values of principal stresses are kept constant [2, 3]. In order to describe these facts the vertex (tangent) effect causing the dependence of not only the magnitude but also the direction of the inelastic stretching on the stress rate has to be incorporated, and thus various constitutive models have been proposed [4, 5, 6]. Among them, the subloading surface model with the tangent effect which incorporates the inelastic stretching, called the tangential stretching, would be applicable to the description of deformation behavior in an arbitrary loading (including unloading and reloading) process of materials with an arbitrary smooth yield surface [6]. In this article the mechanical responses to the stress probe test and the principal stress axes rotation are examined from both aspects of the non-coaxiality induced by the tangent effect and the anisotropy in yield condition, adopting the subloading surface model with the tangential effect and the anisotropic yield surface due to the rotation of yield surface [6, 7]. The signs of a stress (rate) and a stretching (a symmetric part of velocity gradient) components are chosen to be positive for tension, and the stress for soils is meant to be

¹Faculty of Engineering, Kyushu University, Fukuoka, Japan

²Faculty of Agriculture, Kyushu University, Fukuoka, Japan

the effective stress, i.e. the stress excluded a pore pressure from the total stress throughout this article.

Outline of the Subloading Surface Model with Tangent Effect

Tangential Plasticity

The stretching \mathbf{D} is additively decomposed into the elastic stretching \mathbf{D}^e , the plastic stretching \mathbf{D}^p and the tangential stretching \mathbf{D}^t , i.e.

$$\mathbf{D} = \mathbf{D}^e + \mathbf{D}^p + \mathbf{D}^t, \quad (1)$$

where

$$\mathbf{D}^e = \mathbf{E}^{-1} \overset{\circ}{\boldsymbol{\sigma}}, \quad \mathbf{D}^p = \frac{\text{tr}(\mathbf{N} \overset{\circ}{\boldsymbol{\sigma}})}{M^p} \mathbf{N}, \quad \mathbf{D}^t = \frac{\overset{\circ}{\boldsymbol{\sigma}}_t}{T}, \quad \overset{\circ}{\boldsymbol{\sigma}}_t^* = \overset{\circ}{\boldsymbol{\sigma}}^* - \text{tr}(\mathbf{n}^* \overset{\circ}{\boldsymbol{\sigma}}) \mathbf{n}^*, \quad \mathbf{n}^* = \frac{\mathbf{N}^*}{\|\mathbf{N}^*\|}. \quad (2)$$

$\boldsymbol{\sigma}$ is Cauchy stress. ($\overset{\circ}{}$) and ($*$) indicate the proper corotational rate with the objectivity and the deviatoric component, respectively. \mathbf{N} is the normalized outward-normal tensor of the subloading surface f . M^p and T are the plastic modulus and tangential inelastic modulus, respectively. \mathbf{D}^p and \mathbf{D}^t are induced by the stress rate component normal and tangential, respectively, to the yield/loading surface. \mathbf{E} is the fourth-order tensor and given in the Hooke's type as

$$E_{ijkl} = \frac{\nu E}{(1+\nu)(1-2\nu)} \delta_{ij} \delta_{kl} + \frac{E}{2(1+\nu)} (\delta_{ik} \delta_{jl} + \delta_{il} \delta_{jk}), \quad (3)$$

where E and ν are Young's modulus and Poisson's ratio, respectively. δ_{ij} is Kronecker's delta.

Subloading Surface Model with Tangential Effect for Soils

In the subloading surface model the conventional yield surface is renamed the normal-yield surface, since its interior is not regarded as a purely elastic domain. Let the following subloading surface be adopted for soils [8] as

$$f(\boldsymbol{\sigma}, \mathbf{H}) = p(1 + \chi^2) = RF(H), \quad (4)$$

where

$$p \equiv -\frac{1}{3} \text{tr} \boldsymbol{\sigma}, \quad \chi \equiv \frac{\|\hat{\boldsymbol{\eta}}\|}{m}, \quad \hat{\boldsymbol{\eta}} \equiv \boldsymbol{\eta} - \boldsymbol{\beta}, \quad \boldsymbol{\eta} \equiv \frac{\boldsymbol{\sigma}^*}{p}, \quad \boldsymbol{\sigma}^* \equiv \boldsymbol{\sigma} + p \mathbf{I}. \quad (5)$$

R is the similarity-ratio of the subloading surface to the normal-yield surface, where $R=0$ corresponds to the null stress state, $0 < R < 1$ to the subyield state and $R=1$ to the normal-yield state in which the stress lies on the normal-yield surface. The tensor $\boldsymbol{\beta}$ was

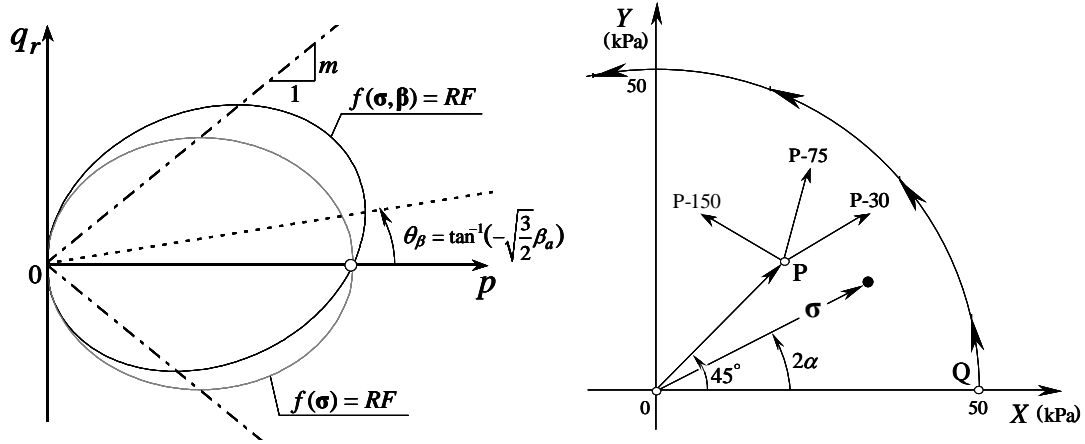


Fig. 1. The subloading surface with rotational hardening. Fig. 2. The stress state in the (X, Y) plane.

introduced in order to describe the anisotropy through the rotation of the yield surface around the origin of stress space (see. Fig. 1). The following evolution equation of the normal-yield ratio R is assumed.

$$\dot{R} = -u \|\mathbf{D}^p\| \ln R \quad \text{for} \quad \mathbf{D}^p \neq \mathbf{0}. \quad (6)$$

The isotropic hardening/softening function F and the rate form of H are given by

$$F = F_0 \exp\left(\frac{H}{\rho - \gamma}\right), \quad \dot{H} = -\text{tr} \mathbf{D}^p, \quad (7)$$

where F_0 is the initial value of F . ρ and γ are material constants describing the slopes of the normal-consolidation and the swelling lines, respectively. The function T in Eq. (2) is assumed in [7] as

$$T = \frac{p}{aR^b \chi^c}, \quad (8)$$

where a , b and c are material constants.

Verification of the Model by Comparison with Experiments under Principal Stress Axes Rotation

The applicability of the present constitutive model to the prediction of deformation behavior for the non-proportional loading in the 2-dimensioal deviatoric stress plane with the axes of the difference of major and minor principal stresses and of the shear stress will be examined based on the simulation of the test results of stress probe [1] and the

principal stress axes rotation tests [2] on Toyoura sand under drained conditions using a hollow cylindrical apparatus.

Test Procedures

In hollow cylindrical test apparatus, four stress components, i.e. the axial stress σ_a , the radial stress σ_r , the peripheral stress σ_θ and the torsional shear stress $\sigma_{a\theta}$ can be applied independently. These four stress components are described by the effective pressure p , the magnitude $\|\sigma^*\|$ of deviatoric stress, the Lode's angle θ_σ and the rotation angle α of the principal stress axes. The state of stress induced in the tests can be also represented in the (X, Y) stress plane (see Fig. 2), where

$$X = \frac{\sigma_\theta - \sigma_a}{2}, \quad Y = \sigma_{a\theta} \quad (9)$$

In the (X, Y) plane, the length of stress vector is equal to the radius of the Mohr's stress circle and makes twice the angle α , i.e. $\tan 2\alpha = Y / X$ (see. Fig. 3).

Stress Probe

The test results for Toyoura sand under the drained condition with constant mean stress [1] are shown in Fig. 4. The three stress increments with the same magnitude $\sqrt{(dX)^2 + (dY)^2} = 15$ kPa at $p=98$ kPa were applied in different directions from the common point P. The inelastic strain increments were calculated by subtracting the elastic components from the total strain increments, whilst the elastic strain increments are calculated by using Young's modulus of $E = 310$ MPa and Poisson's ratio of $\nu = 0.2$, which were determined by experiments [1]. Then, the material parameter γ is determined as $\gamma = 3p(1-2\nu)/E = 0.00057$ for $p = 98$ kPa. The following material constants and initial values are used in the calculation.

$$F_0 = 350 \text{ kPa}, \quad m = 0.96, \quad \rho = 0.0034, \quad \beta_a = -0.15, \quad u = 10, \quad a = 0.01, \quad b = c = 1.0.$$

The calculated and experimental results of the inelastic strain increments for the stress probe from the common stress state P are compared in Fig. 4, whilst the predictions by the four models are depicted by the elastoplastic constitutive models; (a) with neither the anisotropy nor the tangent effect, (b) with the anisotropy due to the rotation of yield surface but without the tangent effect, (c) with the tangent effect but without the

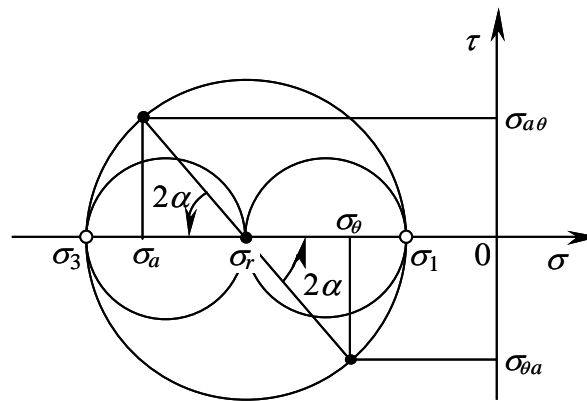


Fig. 3. Mohr's stress circle for the pure principal stress axes rotation.

anisotropy, and (d) with both the anisotropy and the tangent effect. A slight dependence of direction of inelastic stretching on the stress increment is observed in the predictions by the models (a) and (b) without the tangent effect. However, it is caused by the variation in state of stress and thus it is far smaller compared with the test result. It is observed that the model (d) with both the tangent effect and the anisotropy can simulate well the dependence of the inelastic strain increment on the direction of stress increment.

Principal Stress Axes Rotation

The test result [2] for the continuous principal stress axes rotation of $2\alpha = 0$ to 360° from the stress state Q in Fig. 1 keeping $\sqrt{X^2 + Y^2} = 50$ kPa at $p = 98$ kPa is shown in Fig. 5, whilst the same values of material parameters as in the previous section are used. The simulation results by the four models are also shown in this figure. The model (a) predicts only an elastic response. The prediction by the model (c) only with the tangent effect brings about the inelastic strain similar to the test result but the inelastic strain exhibits the completely circular locus and thus diminishes at the end of

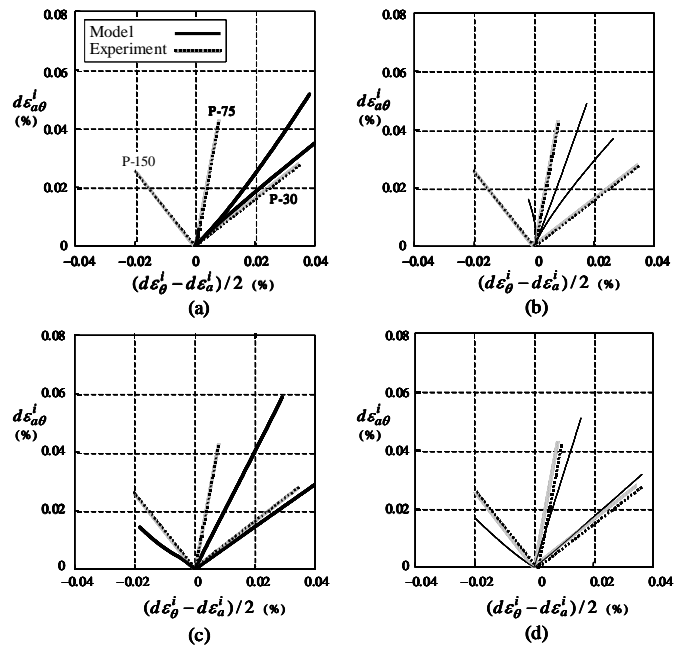


Fig. 4. The inelastic strain increments in the stress probe from the common stress state P.

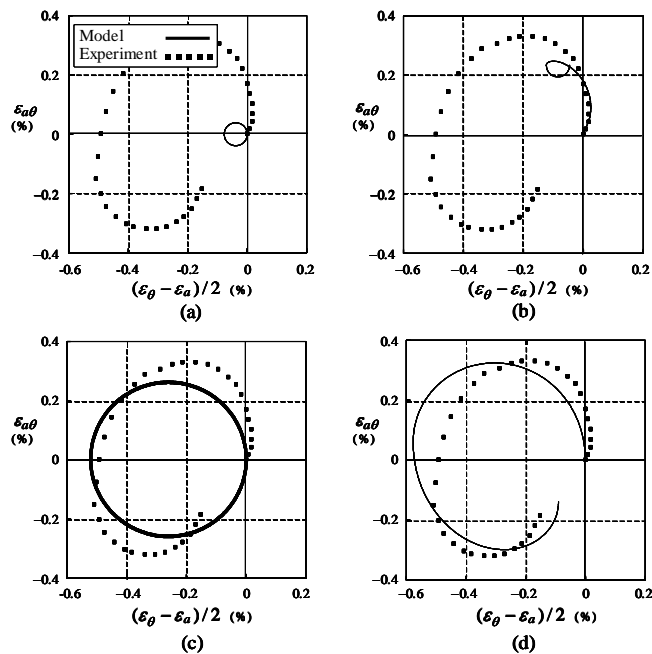


Fig. 5. The inelastic strain in the principal stress axes rotation from the stress state Q.

stress cycle against the test result. The predictions by the model (d) with both the tangent effect and the anisotropy agree well with the test result.

Concluding Remarks

It is verified that the present model has the capability of describing the non-proportional loading behavior of sands by the comparison with the test results for the stress probe and the pure principal stress axes rotation. Eventually, it can be concluded that both the tangent effect and the anisotropy in yield condition have to be incorporated into constitutive equations for the description of general non-proportional loading behavior of soils.

Reference

- 1 Pradel, D., Ishihara, K., Gutierrez, M. (1990): Yielding and flow of sand under principal stress axes rotation. *Soils and Found.* 30(1), pp. 87-99.
- 2 Miura, K., Miura, S. and Toki, S. (1986): "Deformation behavior of anisotropic dense sand under principal stress axes rotation. *Soils and Found.* 26(1), pp. 36-52.
- 3 Gutierrez, M., Ishihara, K., Towhata, I. (1991): Flow theory for sand during rotation of principal stress direction. *Soils and Found.* 31(4), pp. 121-132.
- 4 Rudnicki, J.W., Rice, J.R. (1975): Conditions for localization of deformation in pressure-sensitive dilatant materials. *J. Mech. Phys. Solids* 23, pp. 371-394.
- 5 Papamichos, E., Vardoulakis, I. (1995): Shear band formation in sand according to non-coaxial plasticity model. *Geotechnique* 45, pp. 649-661.
- 6 Hashiguchi, K., Tsutsumi, S. (2001): Elastoplastic constitutive equation with tangential stress rate effect. *Int. J. Plasticity* 17, pp. 117-145.
- 7 Hashiguchi, K., Tsutsumi, S. (2003): Shear band formation analysis in soils by the subloading surface model with tangential stress rate effect. *Int. J. Plasticity* 19, pp. 1651-1677.
- 8 Hashiguchi, K., Chen, Z.-P. (1998): Elastoplastic constitutive equations of soils with the subloading surface and the rotational hardening. *Int. J. Numer. Anal. Meth. Geomech.* 22, pp. 197-227.